A TRNSYS type for the simulation of temperature limiting heat pipe collectors

Julian Jensen, Bert Schiebler and Federico Giovannetti

Institute for Solar Energy Research (ISFH), Emmerthal (Germany)

Abstract

A number of commercially available simulation programs are already able to represent a temperature limitation in solar thermal collectors with a two-part collector efficiency curve. The use of this procedure for the simulation of temperature limiting heat pipe collectors would lead to deviations in its thermal behavior. This work presents a TRNSYS type which is able to represent the temperature limitation of heat pipes in solar thermal collectors correctly. For this purpose, we modified the TRNSYS type 832 regarding the correct temperature limitation behavior. For validation we use measurement data of four demonstration systems with temperature limitation in real operation. The range of consideration includes both flat-plate collectors and evacuated tube collectors with different system dimensions. The comparison shows only minor deviations between simulation and measurement of less than 5 % regarding the solar yield of the collector. Furthermore, the TRNSYS type is used in system simulations and compared to a reference direct-flow collector without temperature limitation, to identify the energetic impact of the temperature limitation onto the solar system performance. By using a direct-flow flat-plate collector, the saved auxiliary energy (f_{save}) increases by +15 %, which has to be considered under the design-related higher aperture area of + 9 %. The use of a direct-flow evacuated tube collector leads to an increased f_{save} of 1.1 %. Additionally, we have investigated the use of both TRNSYS collector types in the IEA SHC Task32 buildings, and reported similar results. The stagnation temperatures > 130 °C were reduced by 600 h and the maximum temperature was reduced by 115 K.

Keywords: solar thermal collector; temperature limitation; heat pipe; system simulation; TRNSYS

1. Introduction

Solar thermal systems are already well-established on the market as efficient renewable heat sources. In 2021, the worldwide installed capacity amounted to 746 million m² with a capacity of 522 GW$_{th}$ (Weiss and Spörk-Dür 2022). High costs and high complexity, however, are major barriers to their dissemination and avoid the development of their large potential. New technical solutions are needed to improve their cost-effectiveness and general acceptance. Novel solar thermal collectors with heat pipes are a promising approach for this purpose. A suitable design provides for a high efficiency in the operating range as well as for the reduction of thermal stress in stagnation state. By using the dry-out effect of heat pipes, the maximum solar circuit temperature can be limited to 125 °C. Preventing overheating in the stagnation state enables cost-effective system configurations with polymeric pipes, smaller designed expansion vessels and cost-optimized solar stations. Furthermore, an easier installation process and low-maintenance operation can lead to a significantly higher profitability of such systems.

In normal operation mode, the incident solar radiation is converted into heat at the collector and then stored in the thermal storage tank. However, if there is no possibility to transfer the heat away from the collector (e.g. if the thermal storage is fully charged) and the solar availability is still high, the state of stagnation occurs. Thus, the solar pump stops its operation and the collector overheats up to its maximum (stagnation) temperature, when the thermal equilibrium is reached. In a usual solar thermal system, this process causes high temperatures and leads to the evaporation of the heat transfer fluid inside the solar circuit. In turn, this leads to high system pressure and to high temperatures in the whole solar system, which can cause significant damage to temperature sensitive components. Conversely, this means that the avoidance of high temperatures during stagnation can increase the lifetime of most system parts and decrease the overall costs due to a simplification in the system design and installation.

The avoidance of critical temperatures during stagnation can be easily accomplished by a collector coverage with an opaque material, however, this must be done by hand and is not beneficial to an efficient system operation. Many other methods have been developed in the past (Harrison and Cruickshank 2012; Frank et al. 2015; Kizildag et al. 2022; Müller et al. 2019) but most of them are not intrinsically safe.

A solution to this problem is the use of heat pipes. These are well-established on the solar thermal market and have been used in evacuated tube collectors for a long time. With the use of special designed heat pipes, the maximum

temperature at the collector can be limited to such an extent that evaporation of the heat transfer fluid can be prevented. This approach has successfully been proved for evacuated tube collectors (Schiebler et al. 2018) as well as for flat-plate collectors (Schiebler et al. 2019).

2. TRNSYS type validation

So far, only one simulation program is known to be able to represent a temperature limitation in solar thermal collectors with the use of a two-part collector efficiency curve (T*SOL (Valentin Software 2022)). Even if this is the right procedure for some temperature limiting techniques (for example thermochromic collectors (Müller et al. 2019)) it does not fit for the heat pipe temperature limitation process and would lead to major deviations in the simulation, since the process is a function of both temperature and irradiance (cf. Fig. 1). For a defined stagnation temperature, the slope of the limitation curve is less steep at high irradiation than at low irradiation, which means, that the performance of the heat pipe collector is stronger affected (limited) at high then at low irradiation.
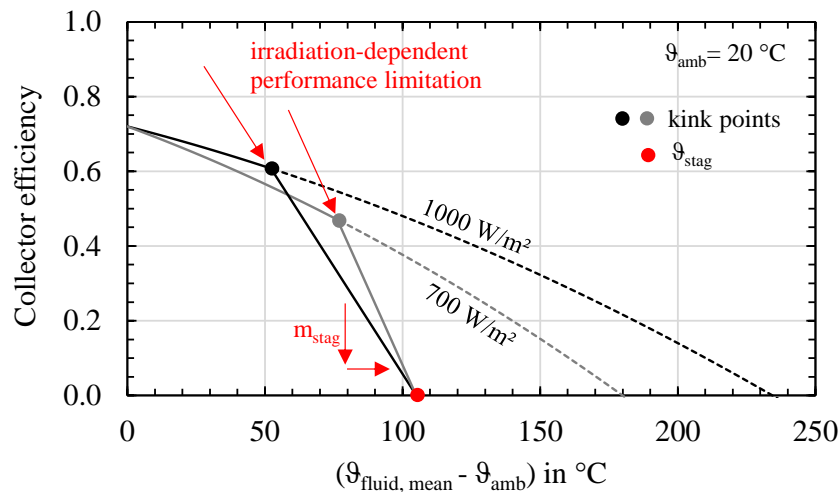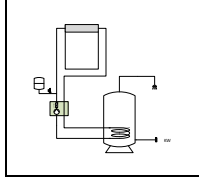

Fig. 1: Collector performance for a standard collector (---) in comparison with a temperature limiting heat pipe collector (-) with variation of the solar irradiance

To be able to correctly simulate temperature limiting heat pipe collectors, we have adapted the TRNSYS type 832 (Haller 2014), which is able to simulate flat-plate collectors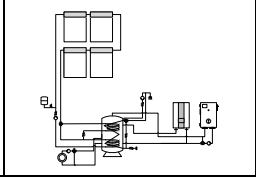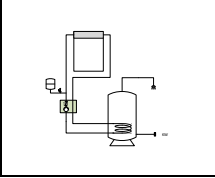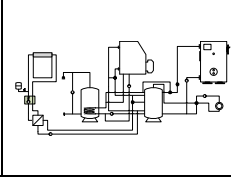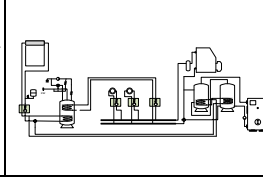 (FPC) as well as evacuated tube collectors (ETC). For this purpose, we have implemented the two parameters ϑ_{Stag} and m_{Stag}, which describes the maximum occurring temperature in the stagnation state and the slope of the heat pipe shut-off function. Both parameters can be identified by means of collector performance measurement, as described in (Schiebler et al. 2018). Since m_{stag} is determined in a power-related measurement, but Fig. 1 shows the efficiency, different slopes result for m_{stag}. The temperature limitation is achieved by limiting the collector efficiency, starting at the so-called kink point. The position of the kink point is dependent on the current irradiation, due to the already mentioned different collector efficiency curves at different irradiation. In order to verify the functionality of this TRNSYS type, the measurement data of real demonstration systems (which are show in Tab. 1 and are also presented in (Schiebler et al. 2022)) were available.

Tab. 1: Overview of the demonstration plants FPC 1-2 and ETC 1-3 with the individual collector area A_{col} (gross area) and heat tank volume V_{tank}

FPC1	FPC2	ETC1	ETC2	ETC3
At institute	**external**	**external**	**external**	**external**

Type: DHW A_{col}: 5 m² V_{tank}: 0.3 m³	Type: Combi A_{col}:20 m² V_{tank}:1 m³	Type: DHW A_{col}:8 m² V_{tank}:0.3 m³	Type: Combi A_{col}:17 m² V_{tank}: 0.15+1 m³	Type: Combi A_{col}: 11 m² V_{tank}: 1 m³+2 m³

These systems have been monitored for more than one year regarding the system performance as well as the temperature distribution in the solar circuit. Fig. 2 shows the comparison between the measurements and the TRNSYS simulations for a chosen day of the FPC2 system by the use of the collector performance. To provide better visibility, the data are presented as a moving average of 2 min. For the sake of comparison, the original TRNSYS type 832 without temperature limitation is also shown. As simulation inputs, we use the measured weather data (irradiation, ambient temperature) as well as the measured collector input temperature.
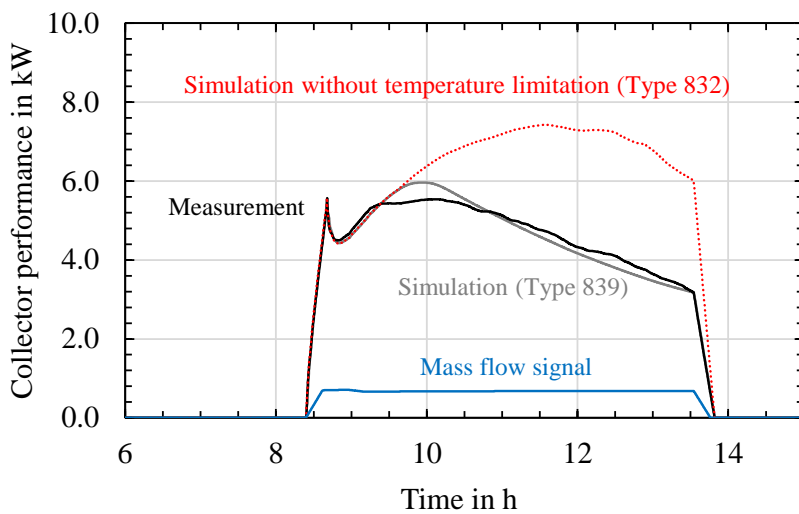

Fig. 2: Moving average (2 min) of the measured collector performance for the FPC2 with heat pipe temperature limitation and comparison of the TRNSYS type 839 with temperature limitation and the TRNSYS type 832 without temperature limitation

The graph shows, that the temperature limitation takes place at around 9:30 am for the measured collector. The simulated start of the temperature limitation is around 10 am. This difference in time occurs due to the ideally simulated collector behavior, which assumes an ideal transition from the working section to the temperature limiting section, which does not correspond to the real operation of a HP collector.

The transition (kink point) from the working section to the temperature limiting section has a huge impact onto the collector simulation, especially if the collector is often operated near to the kink point, as shown in Fig. 3 for the FPC1 system. Here, the simulation exceeds the measured performance due to uncertainties in modeling the limitation process of the heat pipes. The deviations in collector operation should not be neglected at this point and are caused by uncertainties in the measurement system.
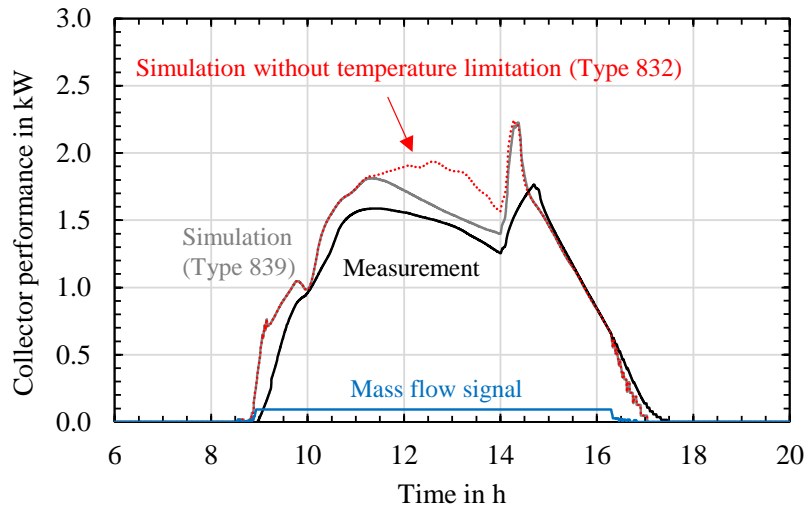
Fig. 3: Moving average (2 min) of the measured collector performance with heat pipe temperature limitation for the FPC1 operated near to the kink point and comparison of the TRNSYS type 839 with temperature limitation and the TRNSYS type 832 without temperature limitation

Furthermore, even small deviations in the heat pipe design and its overall heat transfer coefficient in the collector can lead to a large deviation in the collector behavior, especially in the temperature limiting section. Fig. 4 shows this correlation using the example of an evacuated tube collector.
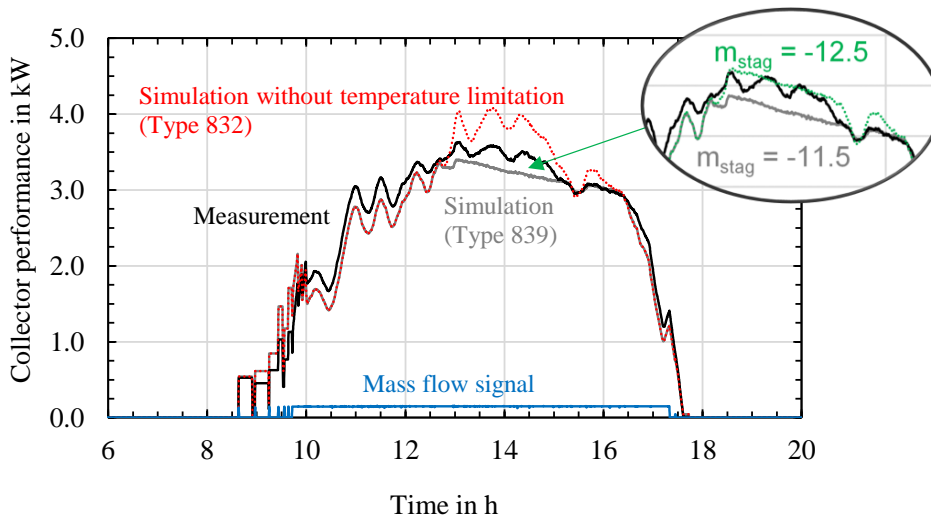

Fig. 4: Moving average (2 min) of the measured and simulated collector performance for ETC3 with heat pipe temperature limitation in comparison with the same collector without temperature limitation (chart) as well as the simulation with a varied parameter of mStag (top right corner)

The deviation can be caused by either a differing heat pipe design, which will cause slightly differing collector parameters, or by the uncertainties of the monitoring system. As shown in the top right corner of the graph, a slightly different value of the parameter m_{Stag} fits the measurement curve in a better way.

In conclusion, the use of the new temperature limiting heat pipe collector TRNSYS type can significantly reduce the deviations between simulation and measurement as it would be the case with the use of the TRNSYS collector type 832. The collector fields of all monitored external systems were also simulated for a period of one month, to investigate the difference between measurement and the simulation with the new TRNSYS type 839. June 2021 was chosen as test period, as it has sufficiently high solar radiation values. Fig. 5 shows the results of the determined solar yields in the observation period. The results are mostly within a satisfactory range of deviation and are in the range of the measurement accuracy of ± 7 % for all plants. The exception to this is the system ETC3, where the radiation measurement (pyranometer) was affected by the shadowing of a near building, which was not considered in the simulation. The FPC1 plant is a laboratory plant at the institute and was operated in the context of dynamic system tests (DST). A comparison of the system yields between the DST approach and TRNSYS is not further discussed here. Furthermore, the simulation results for the TRNSYS type 832 (without heat pipe limitation) are

shown. While the ETC systems experience almost no difference to the TRNSYS type 839 simulation, the result for the FPC system softens a significant increase in solar yield. This can be explained by the fact, that the ETC systems are rarely operated at higher temperatures where the heat pipe limitation takes place. The influence of the annual system yield is discussed later with Fig. 8.
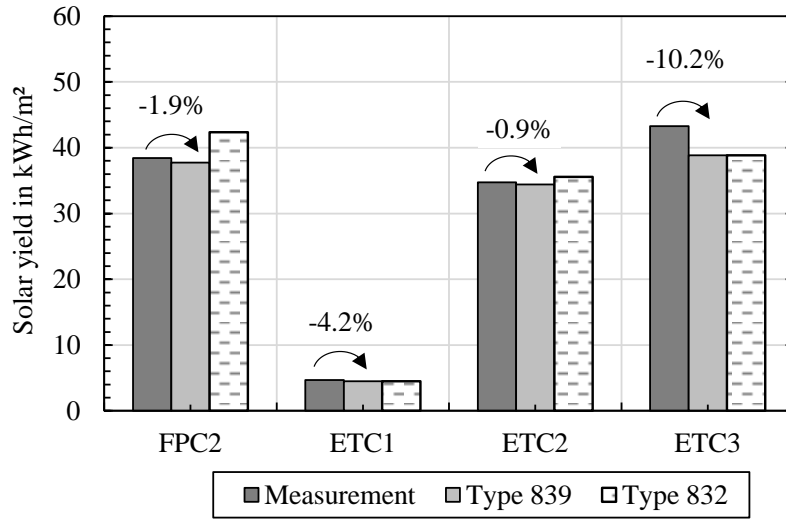

Fig. 5: Evaluation of the thermal gains from the solar thermal collectors in the monitored demonstration systems based on a one-month period (June 2021)

3. System simulations

3.1 Simulation of the monitored demonstration systems

After the experimental validation of the TRNSYS collector type, the monitored systems (solar and heating circuit) were implemented in TRNSYS. For the simulations, we used site-specific Meteonorm 8 weather data (Remund et al.) as well as the system-specific energy demand. The parameterization of the individual components is based on real system parameters. In the case of unknown parameters, standard system assumptions are used. An important parameter for the simulations carried out is the controller of the solar circuit pump, which limits the maximum collector temperature. In a conventional solar thermal system, this value is set to about 125 °C. In the HP system we choose 95 °C which would cause high stagnation times in a normal system. By using temperature-limiting heat pipe collectors and thus preventing steam formation, the operation of the solar circuit pump can be limited to 95 °C without any negative consequences. This allows the use of more cost-effective components and materials, such as polymeric-based piping (Schiebler et al. 2022).

The energetic evaluation of the systems is based on the f_{save} value (Streicher 2003), which expresses the savings in conventional auxiliary energy by the use of a solar thermal system (equation 1). In this equation, $Q_{aux, without ST}$ is the needed energy from the auxiliary heating device if no solar thermal collector is used. In contrast, Q_{aux} indicates the needed energy from the auxiliary heating device with the use of a solar thermal collector.

$$f_{save} = \frac{Q_{aux,without\ ST} - Q_{aux}}{Q_{aux,without\ ST}} \qquad \text{(eq. 1)}$$

The performance of the solar thermal system can be further evaluated via the solar fraction sf (equation 2) by using the solar thermal collector's energy gain Q_{Sol}.

$$sf = \frac{Q_{Sol}}{Q_{Sol} + Q_{aux}} \qquad \text{(eq. 2)}$$

Tab. 2 shows the results of the energetic evaluation of the demonstration plants for the measurement and the simulation. It should be noted that the f_{save} value requires the knowledge of $Q_{aux, without ST}$ which can only be measured for the system ETC1.

The measured data are affected by a measurement accuracy of approx. 7 %. Furthermore, the simulation is based on

average weather data. Both of these issues can cause discrepancies in the simulations. Even if the simulated values (e.g. for Q_{Sol}) are modeled with deviations in comparison with the measured values, the ratios of energy gain and energy demand are appropriate, so that the energetic key figures show only slight deviations from the measured values. It should be noted, that the ETC1 and ETC3 systems are not conventional installations (over- or undersized solar field), which explains the unusual results.

Tab. 2: Comparison between measured and simulated energetic key figures of the monitored systems over a one-year period

			FPC2	ETC1	ETC2	ETC3
Evaluation period			28.07.20 – 27.07.21	05.11.20 – 04.11.21	09.06.20 – 19.05.21	20.05.20 – 19.05.21
Q_{sol}	Measurement	kWh	5258±368	868±61	4451±312	2900±203
	Simulation	kWh	4864	974	4078	2669
f_{save}	Measurement	%	*	82±6	*	*
	Simulation	%	28	80	24	6
sf	Measurement	%	44±3	93±7	25±2	5±0.4
	Simulation	%	37	93	25	5

In the next step, the temperature limiting HP collector was changed with a direct-flow reference collector without temperature limitation. The used collector parameters for the simulations are shown in the appendix (Tab. 3). While the collector parameters for the heat pipe collector are based on a performance measurement carried out in the institute's solar simulator, the reference collector is based on data from a corresponding Solar Keymark certificate (Solar Keymark 2019, 2021). Fig. 6 shows the area specific solar yield for all the investigated systems, both for the use of a HP collector and for the direct-flow collector.
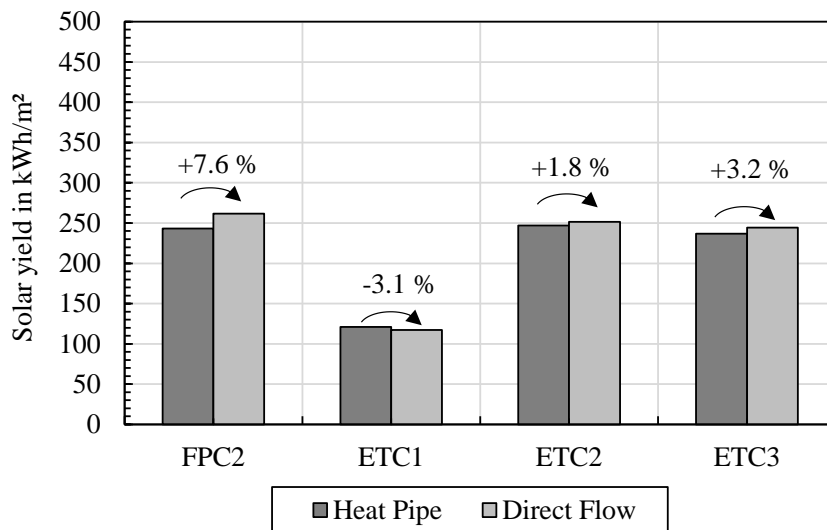

Fig. 6: Area specific solar yield for the investigated systems for both the heat pipe and the direct-flow collector

As expected, the direct-flow collector achieves an additional solar yield for most of the systems. ETC1 has a highly oversized collector area to gain high stagnation times in the system. Due to that, the HP collector can even gain a higher solar yield, caused by the better performance directly after a stagnation event. In general, it can be concluded, that the influence of the HP ETC onto the solar yield is lower than it is for the FPC. This is caused by the approximately 9 % smaller aperture area of the HP FPC in comparison with the HP direct-flow collector. Furthermore, the lower aperture area has a higher influence onto the saved auxiliary energy (f_{save}), as can be seen in Fig. 7. While the increase in the f_{save} - value remains about the same for the ETC, it increases significantly to 14 %

for the FPC. This correlation was also confirmed by parallel DST measurements at the institute's demonstration system FPC1 (Schiebler et al. 2022).
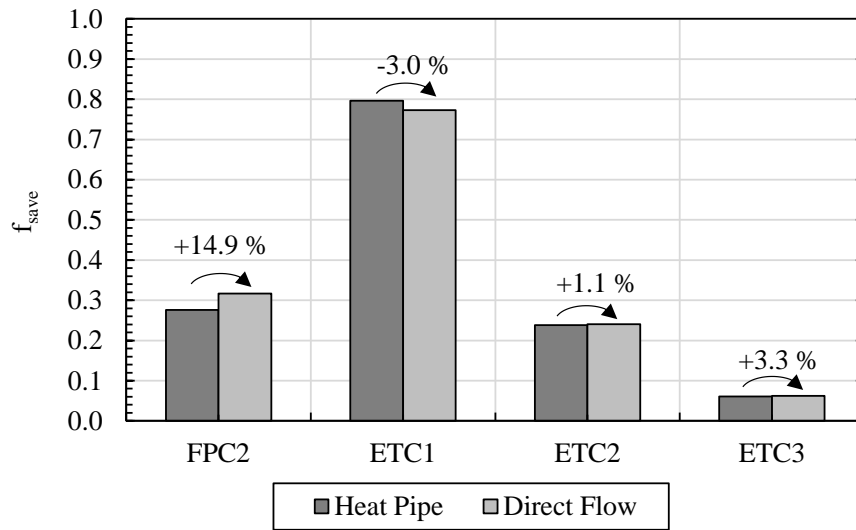

Fig. 7: Saved auxiliary energy due to the use of both the heat pipe collector and the direct-flow collector

In order to evaluate the results regarding the influence of the heat pipe limitation, we varied the maximum collector temperature ϑ_{Stag} (cf. Fig. 1) for all systems. Fig. 8 shows the simulated f_{save} value for each of the monitored systems in comparison with a heat pipe collector without temperature limitation (equivaltent to TRNSYS type 832). As it can be seen, the influence of the limitation process can be neglected for maximum temperatures of $\vartheta_{stag} > 120$ °C, which is the case for the ETC heat pipe collector in the demonstration systems. For $\vartheta_{stag} < 120$ °C, the heat pipe limitation starts to affect the f_{save} value, but in a small manner. It should be stated out, that the simulation of maximum temperatures of less than 100 °C is a pure hypothetical study, as the heat pipe process would not be functional in this way in real operation.
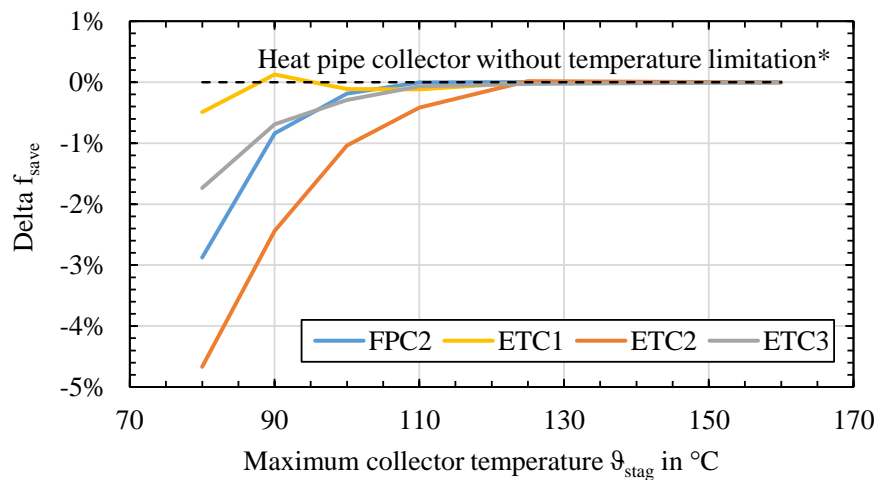

Fig. 8: Change of f$_{save}$ due to the variation of the maximum collector temperature in comparison with a heat pipe collector without temperature limitation (*equivalent to TRNSYS type 832)

In summary, the given results indicate, that the solar yield of the simulated systems is not significantly affected by the heat pipe limitation and thus TRNSYS type 832 could also be used for its simulation without making any major errors. However, this statement must always be considered in the context of differing system configurations, which has a huge influence of the occurring collector temperatures and thus onto the influence of the heat pipe limitation. To correctly simulate the temperature limiting heat pipe collector, TRNSYS type 839 is needed.

3.2 Simulation of Task 32 building

In addition to the real demonstration systems, the corresponding collectors were simulated for two buildings of the IEA SHC Task 32 (Heimrath and Haller 2007) to achieve a better comparability by using a representative building with a customary solar system. The buildings represent a single-family house with a space heating demand of 45 kWh m^{-2} a^{-1} (SFH45) and 100 kWh m^{-2} a^{-1} (SFH100) at the Zürich site. These systems are simulated with both FPC and ETC, each in the HP and reference configuration (parameters are shown in Tab. 3 in the appendix). They consist mainly of 20 m² collector gross area and a 900 l thermal storage tank with a gas boiler as auxiliary heating.

Fig. 9 shows the distribution of the occurring collector temperatures for a one-year based simulation with the SFH45 building for an ETC on the Würzburg site. As it can be seen, the reference collector is exposed to temperatures above 130 °C, which accumulates for around 400 h per year with a maximum temperature of slightly above 240 °C. In contrast, the stagnation temperatures of the HP collector are switched to the 120 – 130 °C interval, since its maximum temperature is 125 °C. This equals a reduction of the maximum occurring temperature of 115 K. If this simulation is performed with TRNSYS type 832 (as discussed before), the frequency for temperatures above 130 °C would accumulate for around 600 h (which is higher than the frequency of the reference collector, since the controller shut-off is 95 °C for the HP collector). For the SFH100 building and other locations, the collector temperature distribution shows a similar pattern but with differing frequencies.
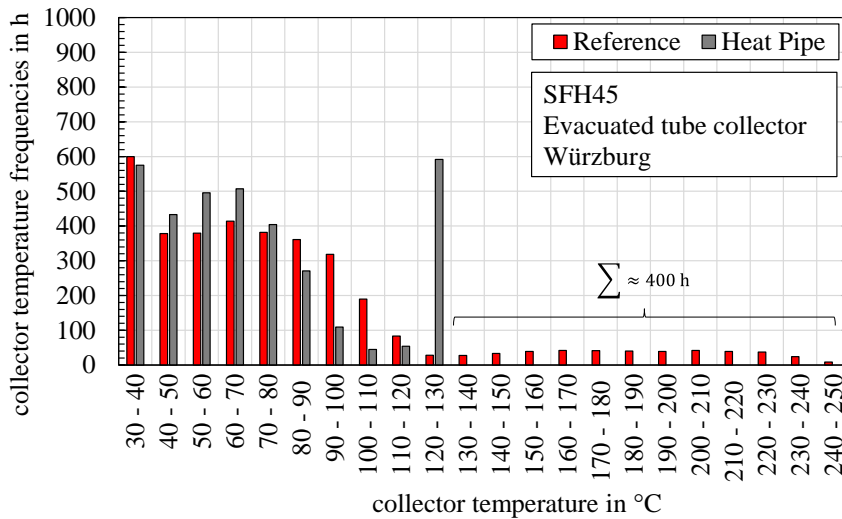

Fig. 9: Overall collector temperature frequencies for a simulation of the SFH45 building with 20 m² ETC collector gross area on the Würzburg site

Furthermore, we have compared the reference collector with the HP collector regarding the f_{save} value to evaluate the energetic impact of the temperature limitation. As it is shown inFig. 10, by using the flat-plate reference collector, the f_{save} value increases by 9.6 % for the SFH100 building at the Würzburg site. This result correlates very well with the 9% higher aperture area of the reference collector. For the SFH45 building, the increase is only 6.8 %, because stagnation and standstill effects of the collector occur more frequently, due to the lower space heating demand.

By using the evacuated tube reference collector, the increase in the f_{save} value is even lower (3.9 %), since higher collector temperatures are reached faster and thus the influence of stagnation and standstill effects is also larger.

In principle, an analogous behavior can be observed for the Athens site, but at a lower level of increase.

In general, the simulation of the Task32 buildings show similar results to our monitored demonstration systems (ETC less influence than FPC), but can extend this investigation to include other location. Especially for a location with high solar incidence (e.g. Athen), the energetic impact of the HP collector is small while at the same time, a temperature limitation is accomplished that can fully prevent stagnation.
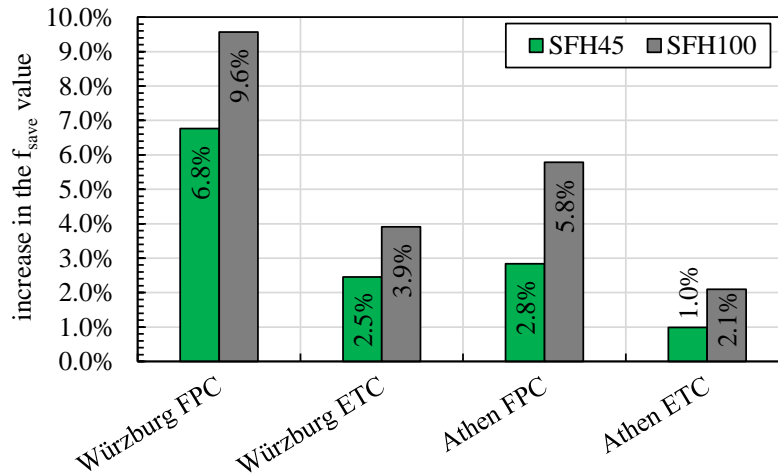
Fig. 10: Increase in the f$_{save}$ value by replacing the temperature limiting HP collector with the direct-flow reference collector without temperature limitation

4. Conclusion

We simulated four solar thermal demonstration plants with temperature limiting heat pipe collectors (HP) in the TRNSYS simulation environment. For this purpose, the existing TRNSYS type 832 was adapted regarding the heat pipe based temperature limitation and validated on the basis of measurement data from the demonstration plants. Measured boundary conditions (radiation, inlet temperature, mass flow and other environmental conditions) were read into the model and the simulated collector performance was compared with the measured one. The heat pipe limitation is well reproduced, only in the kink point region there are small deviations, which are caused by the ideal model description and small uncertainties in the HP collector design. For an evaluation period of one month (June 2021), the deviation does not exceed 5 %.

After the model validation, we performed annual simulations with synthetic weather data and energy consumptions in TRNSYS. The aim of this simulation was to analyze the behavior of the systems when using different collectors (temperature-limited heat pipe collectors as well as direct-flow reference collectors). We evaluated the quality of the simulation based on the comparison between simulation and measurement. The resulting deviations increase with the complexity of the overall system, but are within a satisfactory range, considering the occurring measurement accuracy.

Based on these models, different parameter variations were performed and energetically evaluated. The replacement of the temperature-limiting heat pipe collector with a direct-flow reference collector was presented. For the two system configurations we report different results. In the flat-plate collector system presented, the use of the reference collector leads to an increase in conventional energy savings (f_{save}) of about 15 %. The reason for this, however, is not the shut-off behavior of the heat pipe, but rather its smaller aperture area of approx. 9 % due to the design, as well as the higher heat resistances in connection with the use of heat pipes. For the evacuated tube collector system, the f_{save} value increases by only 1.1 % when a direct-flow reference collector is used.

The simulations were also performed with the TRNSYS collector type 832 with the same collector parameters but without the heat pipe temperature limitation. The influence onto the solar yield is neglectable small (for the investigated systems) but high stagnation loads are simulated. Thus, TRNSYS type 832 could also be used for the simulation of the investigated systems without making any major errors regarding the solar yield but to correctly simulate the temperature limiting heat pipe effect, TRNSYS type 839 is needed.

Finally, two representative single-family buildings (SFH45 and SFH100), which were defined in the IEA Task 32, were simulated with both of the collectors. These simulations report similar results to those obtained during the simulation of the demonstration systems and confirm the essential statements of our experimental investigations, especially with regard to the differences between HP collector and reference collector as well as the influence of the shut-off temperature on the annual yield. We showed, that for the Würzburg site a significant reduction of the stagnation load of 400 h can be achieved by using the HP collector. Thereby the maximum temperature was reduced by 115 K from 240 °C to 125 °C.

Literature Cited

Frank, E., Mauthner, F., Fischer, S., 2015. Overheating prevention and stagnation handling in solar process heat applications. IEA SHC Task 49.

Haller, M., 2014. TRNSYS Type 832 v5.10 „Dynamic Collector Model by Bengt Perers" Updated Input-Output Reference. Rapperswil, Switzerland.

Harrison, S., Cruickshank, C. A., 2012. A review of strategies for the control of high temperature stagnation in solar collectors and systems. Energy Procedia 30, 793-804.

Heimrath, R., Haller, M., 2007. The Reference Heating System, the Template Solar System of Task 32.

Kizildag, D., Castro, J., Kessentini, H., Schillaci, E., Rigola, J., 2022. First test field performance of highly efficient flat plate solar collectors with transparent insulation and low-cost overheating protection. Solar Energy 236, 239-248.

Müller, S., Giovannetti, F., Reineke-Koch, R., Kastner, O., Hafner, B., 2019. Simulation study on the efficiency of thermochromic absorber coatings for solar thermal flat-plate collectors. Solar Energy 188, 865-874.

Remund, J., Müller, S., Schmutz, M., Graf, P. Meteonorm Version 8. EUPVSEC 2020 online conference 07. - 11. September 2020.

Schiebler, B., Jack, S., Dieckmann, H., Giovannetti, F., 2018. Experimental and theoretical investigations on temperature limitation in solar thermal collectors with heat pipes: Effect of superheating on the maximum temperature. Solar Energy 171, 271-278.

Schiebler, B., Köhler, J., Wagner, L., Jensen, J., Giovannetti, F., 2022. Heat Pipe Collectors with Overheating Prevention in a Cost-Optimized System Concept: Monitoring of System Performance and Stagnation Loads under Real Conditions. EuroSun Conference, Kassel, Germany, 25-29 September (in press).

Schiebler, B., Weiland, F., Giovannetti, F., Kastner, O., Jack, S., 2019. Improved Flat Plate Collector with Heat Pipes for Overheating Prevention in Solar Thermal Systems. ISES Solar World Congress 2019/IEA SHC International Conference on Solar Heating and Cooling for Buildings and Industry 2019, Santiago, Chile, 3- 8 November.

Solar Keymark, 2019. Flat Plate collector KBB K420-DH: License number 011 - 7S323 F.

Solar Keymark, 2021. Evacuated Tube Collector ELCO Auron DF: Licence number 011-7S2979 R.

Streicher, W., 2003. Report on Solar Combisystems Modelled in Task 26 (System Description, Modelling, Sensitivity, optimisation): A technical report of Subtask C.

Valentin Software, 2022. T*SOL - The design and simulation software for solar thermal systems. Accessed Jul 26, 2022. https://valentin-software.com/en/products/tsol/.

Weiss, W., Spörk-Dür, M., 2022. Solar Heat Worldwide: Global Market Development Global Market Development and Trends 2021 Detailed Market Figures 2020. Gleisdorf, Austria.

Appendix

Tab. 3: Used collector parameters for the temperature limiting HP collector and the reference collector without temperature limitation for both the FPC and the ETC

Parameter	Unit	Flat-Plate (FPC)		Evacuated tube (ETC)	
		Heat Pipe (HP)	Reference (Ref)	Heat Pipe (HP)	Reference (Ref)
-	-	Measurement	011-7S323F	Measurement	011-7S2979 R
η_0	-	0.748	0.856	0.72	0.772
K_{diff}	-	0.870	0.870	0.920	0.88
a_1	W m^{-2} K^{-1}	3.940	3.710	1.9	1.403
a_2	W m^{-2} K^{-2}	0.0136	0.016	0.005	0.011
U_{int}	W m^{-2} K^{-1}	21	67	16	127
c_{abs}	J m^{-2} K^{-1}	4900	3179	1590	932
c_{fluid}	J m^{-2} K^{-1}	1350	2657	3160	5397
m_{Stag}	W m^{-2} K^{-1}	-13.0	-	-11.5	
T_{max}	°C	110 / 125 / 160	210	110/ 125 / 160	280
$A_{aperture}$	m²	2.12	2.3	1.01	1.01
A_{gross}	m²	2.51	2.51	1.61	1.61

Tab. 4: Used symbols and their quantities

Quantity	Symbol	Unit	Quantity	Symbol	Unit
area	A	m^2	auxiliary energy needed without the use of a solar thermal collector	$Q_{aux,without ST}$	kWh
linear heat loss coefficient	a_1	W m^{-2} K^{-1}	solar thermal yield	Q_{sol}	kWh
quadratic heat loss coefficient	a_2	W m^{-2} K^{-2}	specific solar thermal yield	q_{sol}	kWh m^{-2}
collector specific heat capacity without fluid	c_{abs}	J m^{-2} K^{-1}	solar fraction	sf	%
collector fluid specific heat capacity	c_{fluid}	J m^{-2} K^{-1}	internal heat transfer coefficient	U_{int}	W m^{-2} K^{-1}
solar irradiation	E	kW h m^{-2}	Volume	V	m³
saved auxiliary energy by the use of a solar thermal system	f_{save}	%	inclination angle (0° = horizontal)	α	°
incidence angle modifier for diffuse radiation	K_{diff}	-	zero-loss coefficient	η_0	-
slope of heat pipe power shut-off	m_{stag}	W m^{-2} K^{-1}	temperature	ϑ	°C
auxiliary energy needed in a solar thermal system	Q_{aux}	kWh			